AIAA 80-1277R

Nozzleless Boosters for Integral-Rocket-Ramjet Missile Systems

I. M. Procinsky* and Catherine A. McHale†
Atlantic Research Corporation, Gainesville, Va.

The concept of a nozzleless solid-propellant booster for an integral-rocket-ramjet missile system offers a number of advantages over the conventional ejectable-nozzle design. These advantages include elimination of the debris hazard, simplicity of design, reliability, and performance. Experience with both subscale and full-scale motor designs shows that with a grain length to diameter ratio of 3.5, a nozzleless booster will match the performance of an ejectable-nozzle system, and that at larger ratios the nozzleless motor can be configured to produce up to 15% greater performance. General design rules and limitations are also presented.

Introduction

DURING the last six years, our organization has been funded to perform a number of model studies and test programs aimed at developing nozzleless boosters for integral-rocket-ramjet systems. This work has been performed with the goal of characterizing the behavior and comparing the performance of various nozzleless booster configurations. The motor programs and analytical studies span the full range of tactical and strategic air launched systems and include the use of reduced smoke, aluminized, and high-density zirconium-loaded propellant formulations.

In the implementation of these programs, over 250 nozzleless rocket motors, many of them containing integral-rocket-ramjet-nozzle inserts, having been functionally tested. Boosters ranging in size from 3.5 to 20.0 in. in diameter have been fired to provide a data base for the evaluation and modification of the nozzleless internal ballistics code that is used as the primary design tool for new system applications.

A sufficient number of combinations of propellant systems and motor configurations have been tested so that there are enough empirical data to allow extrapolation with assurance that the accuracy of the ballistics predicted by the model will fall within 0.5-2.5%. Therefore, the data presented are based on a model that is not as precise as the available nozzled ballistics program, which are generally twice as accurate as the current nozzleless program. This difference is due primarily to the relative complexity of the phenomena that control the behavior of a nozzleless motor and partly to the fact that nozzleless technology is a relatively new field. Work on a second-generation prediction model, which will be more theoretically based and much less dependent on empirical constants, has begun and will be completed next year.

Background

The concept of a nozzleless solid-propellant rocket motor was revived about 10 years ago in an attempt to produce a simpler and therefore more-economical rocket motor. It was then anticipated that the elimination of the nozzle assembly, the reduction of case insulation requirements, and the relative simplicity of the grain configuration would lead to a net production-cost saving on the order of 10-20%.

Initial experimental data showed that, for a given external motor geometry, the lower operating efficiency of the nozzleless configuration could, in most instances, be compensated by filling the volume previously occupied by the nozzle assembly with propellant. Usually, this higher-mass-fraction configuration would almost match the velocity increment produced by a similarly sized nozzled motor. Failure to achieve comparable performance in the initial experiments was attributable to insufficient propellant burn rate and structural characteristics.[1]

The properties of an ideal propellant for a nozzleless configuration have to be significantly different from those of a nozzled motor. With the exception of motor envelopes of high length-to-diameter ratio (15/1 or greater), the burning rate of the propellant must be higher in order to prevent a long and inefficient tail-off and the physical properties at both ends of the operating temperature range must also be better. At low temperature, the strain capacity has to be superior in order to allow optimum web fraction, propellant loading, and total performance. At high temperature, the stress capacity has to be higher so that the grain structure can survive the shear loads produced by the large axial pressure differential between the head-end and aft-end of a burning nozzleless grain.

One consequence of these effects is that propellant ingredient and development costs are typically higher for a nozzleless motor.

This does not mean to imply that the characteristics required of a nozzleless propellant are impossible to obtain. Formulations meeting program goals have been successfully produced for all of the nozzleless programs undertaken thus far. It does mean, though, that the current limited demand for many of the ingredients, and the resulting higher processing costs, tend to offset some of the cost advantage of the nozzleless design. In spite of these factors, a straightforward nozzleless booster can be designed to yield comparable performance at a price reduction of about 10%, and a performance gain of up to 15% is possible if the propellant strength and burning-rate/pressure exponent can be optimized.

More recently, the resurgence of interest in air-breathing systems has led to programs aimed at adapting the nozzleless approach to a system in which considerations other than cost and ease of manufacture predominate.

On all programs initiated before 1976, the integral-rocket-ramjet (IRR) booster design called for an ejectable nozzle apparatus. A number of such systems have been developed and successfully demonstrated in ground tests and in a limited number of flight tests.[2]

The ejectable nozzle approach as depicted by Fig. 1 presents a number of complications and penalties to the performance of a ramjet. Past problems include leakage between the ejectable nozzle and the ramjet nozzle, the need to add significant structural supports, failure of the separation mechanism, control circuitry and logic, and general reliability considerations.

Presented as Paper 80-1277 at the AIAA/SAE/ASME 16th Joint Propulsion Conference, Hartford, Conn., June 30-July 2, 1980; submitted July 24, 1980; revision received Dec. 29, 1980.

*Head, Motor Technology Section, Advanced Projects Dept., Propulsion Div.

†Project Engineer, Motor Technology Section, Advanced Projects Dept., Propulsion Div.

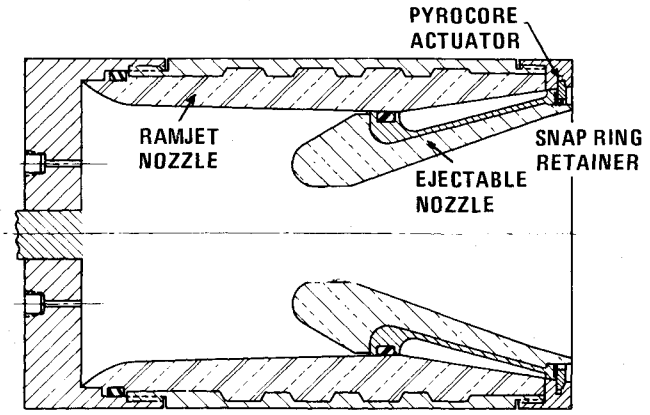

Fig. 1 Ejectable-nozzle test assembly.

Advantages of Nozzleless IRR Configuration

Until the development of the nozzleless IRR booster, the ejectable nozzle represented the most practical system. Consequently, most of the problems relating to the ejectable nozzle have been solved. The one that has not been solved is the possibility of collision between solid ejecta from the missile and the launching aircraft. The nozzleless design appears to provide a solution to this problem.

The elimination of the ejectable nozzle system by itself represents considerable advantage in an air-launched ramjet booster, but there are a number of additional factors that reinforce this choice. These include 1) simplicity, 2) reliability, 3) mass fraction, and 4) cost.

The nozzleless IRR booster depicted in Fig. 2 has no moving parts. It does not require redundant control circuits and actuators. It is inherently simpler, more reliable, and does not require additional aft-combustor structural supports. The nozzleless grain burns out evenly, which means that there is no localized erosion of the combustor insulation. Similarly, the integral ramjet nozzle remains covered during most of the booster burn. Full-scale tests of different IRR boosters with silica phenolic ramjet nozzles show negligible erosion during booster burn. The elimination of the ejectable nozzle also removes the possibility of damaging the IRR nozzle during the separation event or by leakage before the separation.

One nozzleless motor advantage, which may or may not be important for all applications, is cost. The ejectable nozzle and its attendant components represent a sizable fraction of booster production costs. In addition, a nozzled grain design usually requires grain slots that make casting hardware more expensive. It is therefore relatively easy to show that a cost trade-off between an ejectable nozzle design and the additional propellant needed by a nozzleless design will favor a nozzleless configuration.

The final advantage, and the one that overshadows the others in importance, is motor performance. Historical motor data and model studies indicate that depending on how successful one is in optimizing the critical characteristics of the propellant, and depending on how high a length-to-diameter ratio the combustor case will allow, the nozzleless design will yield anywhere from a 2 to 15% increase in velocity increment over a comparable geometry nozzled design.

Constraints

There are certain complications associated with a nozzleless motor. The conversion from a nozzled to a nozzleless design requires more than a change in the shape of the propellant grain. The propellant used in the nozzleless configuration must typically have a higher burning rate and better physical properties in order to achieve comparable performance. Combustor envelope configurations of low length-to-diameter ratio ($<3.5/1.0$) will generally result in a performance penalty.

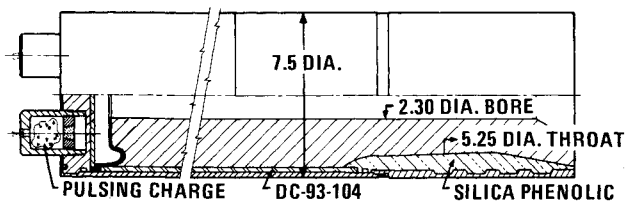

Fig. 2 Nozzleless-booster test configuration.

Finally, improved performance is usually achieved by filling the volume previously occupied by the nozzle with propellant. Since the weight of the additional propellant may be higher than the weight of the ejectable nozzle apparatus, the nozzleless design will produce more impulse, but may also have a higher launch weight.

Review of Nozzleless Technology

The following material begins with a description of the first generation internal ballistics model that is used to design nozzleless motors and continues with a presentation of historical motor data and an evaluation of the basic parameters that control the performance of nozzleless motors. The section concludes with an assessment of the accuracy of the model.

Internal Ballistics Model

The first generation Nozzleless Rocket Motor Internal Ballistics Computer Program has been in existence since 1973.[3] This program has been used since then to design nozzleless motors and generate parametric studies for numerous rocket motor applications.

Initial attempts to use this program made it obvious that the program had a number of deficiencies and limitations. Since then, much has been done to modify and correct the computer model. During the last 2 years, this work has led to a number of improvements and the publication of a revised manual.[4]

The changes, along with experience gained in using the program, have resulted in a model that will run on the first attempt with run time reduced, in most instances, to less than 20 s.‡

The prediction program has been developed to the point where initial grain geometry is no longer a limitation and where the computational logic errors have been corrected so that it will run within the analytical constraints of the specified equations. However, a number of phenomena, which according to historical data are not well enough understood to allow their precise definition, still limit the accuracy of the computer routine and force the user to rely heavily on empirical corrections. The questionable phenomena include the following: 1) combustion efficiency, which relies on single-particle trajectory correlations; 2) erosive burning, which depends on a strictly empirical fit; 3) grain deflection, which uses a simplified linear correlation from static calculations; 4) nozzle separation, which can occur with over-expanded exit cone cases, and which is not treated at all.

The lack of more precise handling of these phenomena forces the program to rely on the specification of approximately 15 empirical constants. Although there is an analytical basis for specifying values for some of the constants, there is no way other than applying empirical corrections based on motor experience to define combinations of values that will result in an unproved fit. As expected these constants are strongly dependent on motor geometry, propellant composition, physical properties, and temperature. In spite of these limitations, it is possible to obtain accurate ballistics predictions, but the accuracy obtained depends significantly on the amount of similar motor data available for correcting the empirical constants.

‡CPU time on IBM 370/168 computer.

Table 1 A priori model comparison

Case	Configuration	Propellant	Diameter	Prediction error				
				P_{max} %	F_{max} %	Action time, %	Total impulse, %	Specific impulse, %
9	Cylinder/ restricted aft-end	HTPB/reduced-smoke	4	−1.4	+2.0	+0.4	+0.3	+0.2
19	IRR booster	HTPB/zirconium	8	−1.4	−2.7	+4.2	+0.6	+0.7
15	IRR booster	HTPB/reduced-smoke	7	+3.1	−11.3	+5.0	−0.6	+0.3
1	IRR booster	HTPB/aluminum	18	+22.0	+8.8	−8.4	+1.9	+1.0

Table 2 Historical motor performance summary

Case number	Configuration	Propellant	Diameter, in.	Motor length, in.	Grain length/diameter	Web fraction	P_{av}, psia	I_{sp}^{a}, %
1	Integral rocket ramjet booster (IRR)	HTPB/Al	18	60.0	3.4	0.69	365	78
2	Cylinder	HTPB/Al	6	34.0	5.9	0.65	880	76
3	IRR	HTPB/Al	6	34.0	5.9	0.65	1050	82
4	Cylinder, no exit cone	HTPB/Al	5	34.0	7.6	0.60	400	76
5	Cylinder	HTPB/Al	5	34.0	7.6	0.60	340	81
6	Cylinder	HTPB/Al	6	34.0	6.1	0.62	330	79
7	Cylinder	HTPB/Al	13	100.0	7.7	0.40	1325	80
8	Cylinder	HTPB/Al	6	34.0	5.6	0.40	650	71
9	Cylinder, aft restriction	HTPB/reduced-smoke	4	52.0	13.9	0.67	800	80
10	Cylinder	HTPB/reduced-smoke	5	34.0	6.8	0.60	210	68
11	Cylinder	HTPB/reduced-smoke	4	52.0	13.9	0.67	700	80
12	Cylinder, aft restriction	HTPB/reduced-smoke	4	52.0	13.9	0.67	930	82
13	IRR	HTPB/reduced-smoke	7	42.0	5.8	0.67	300	79
14	IRR	HTPB/reduced-smoke	7	45.0	6.7	0.65	870	84
15	IRR	HTPB/reduced-smoke	7	45.0	6.7	0.65	480	81
16	Cylinder	HTPB/reduced-smoke	6	34.0	7.6	0.60	380	77
17	Cylinder, no exit cone	HTPB/reduced-smoke	6	34.0	7.6	0.60	330	71
18	IRR	HTPB/zirconium	7	50.0	6.9	0.70	430	76
19	IRR	HTPB/zirconium	8	39.0	5.2	0.67	510	75

[a] The specific impulse values are listed as percentages of the delivered specific impulse obtainable from an optimum-design nozzled motor using a similar propellant.

Accuracy of Model

More than 1800 computer runs have been made by our organization using the ballistics prediction program to generate models of nozzleless motors. At least ten significantly different motor configurations, utilizing five different propellant systems, have been fired.

The large number of configuration/propellant combinations that have been tested have provided an opportunity to make numerous pre-test predictions and post-test adjustments of the empirical constants that control the accuracy of the model output. The results show that erosive burning, grain deflection, and flow separation all have effects that must be empirically adjusted in this first generation model in order to generate usable results.

Considering the number and complexity of the phenomena involved, the basic nozzleless model described in the revised manual does well in predicting overall performance if one properly selects the constants that have been found to be critical: erosive burning, radial grain deflection, particle size for any metal ingredient present, and an artificial combustion temperature reduction to compensate for incomplete combustion. Without any motor experience, the ballistics prediction will, in general, be accurate to within 3-4% on total impulse and burn time. Ignition pressure will usually be the most inaccurately predicted value and can be in error by as much as 15%. The shape of the ballistics curves will show maximum variations in the 5-8% range, but even these prediction accuracies require the definition of three erosive constants.

If nozzleless motor firing data with a similar propellant formulation, but not necessarily a similar motor geometry, is available, the accuracy of prediction can be improved to between 1% and 1.5% for total impulse and burn time, and to better than 5% for the other ballistic parameters. As will be shown, the model does demonstrate a-priori prediction accuracy sufficient to make it a useful design tool. Table 1 summarizes the results obtained for three basic propellant systems. The case numbers refer to the configurations defined in Table 2.

As shown in Table 1, the model accuracy is good for overall performance parameters such as total and specific impulse. The largest errors appeared in case 1, which represented the first attempt at firing a large, nozzleless booster. These values represent a-priori prediction attempts, which were subsequently adjusted, as additional analytical and test data became available, to levels below those indicated previously.

It can be concluded, therefore, that sufficient empirical data exist to define the limitations of the internal ballistics computer program and that this program can be used to produce meaningful designs of future nozzleless booster systems.

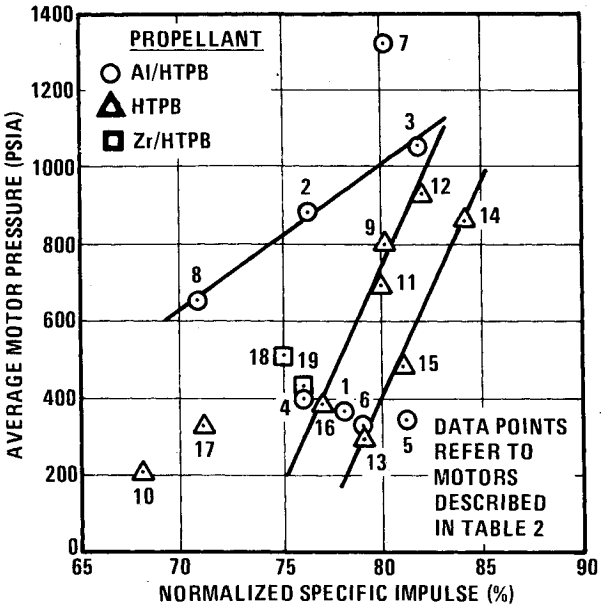

Fig. 3 Normalized specific impulse vs average motor pressure.

Evaluation of Historical Motor Data

As mentioned previously, the performance of a nozzleless booster depends on the success one has in optimizing the physical properties and burning rate of the propellant.

In many instances, the outer envelope of the grain is already defined by the combustor geometry, and the only variables available to the designer are the propellant composition, propellant burning rate, and the shape of the bore of the grain. These variables, in themselves, are usually more than sufficient to allow appropriate tailoring of the ballistics. However, as the motor ballistics show, there are a number of basic relationships which limit the performance that can be obtained with a particular geometry.

The data presented in Table 2 and Fig. 3 represent a range of geometries and operating conditions covering the range of historical motor data for three different propellant systems: one nonmetallized and two metallized systems. The differences in propellant formulation between members within each of the three groups are not large enough to prevent comparison of performance within each group.

The first group of eight motors listed in Table 2 was loaded with state-of-the-art, high solids, aluminum/HTPB propellant. Case 1 is an 18-in. diameter, 60.0-in.-long motor with an integral ramjet throat and a 0.69 web fraction. It developed a specific impulse of 78%§ of the reference value at an average operating pressure of 365 psia and came within 2% of matching the total performance of a nozzled booster in the same envelope. Performance comparability requires that the additional propellant compensate for the difference in specific impulse that a similar nozzled motor will deliver. Such a value is typical of nonoptimal nozzleless configurations. In many instances, a nozzleless motor recovers only 70-75% of the theoretical impulse available from the propellant. The 25-30% differential between ideal and measured specific impulse is due primarily to the lack of a fixed nozzle and exit cone for expanding the exhaust. Although a nozzleless motor begins operating with an expansion ratio of less than 8.0 at ignition, this ratio drops exponentially to 1.0, or in the case of an integral ramjet booster, at best to a value of 2.0 at web burnout.

Another major contributor to the performance shortfall is the low operating pressure during the last half of a nozzleless burn. Although a nozzleless motor begins operating at a high pressure, at web burnout the pressure can be as low as 15% of the ignition maximum, and even though the IRR throat provides some choking at the end of the burn, the average operating pressure and therefore the net combustion efficiency of the burn suffers.

There are a number of ways to compensate for these problems. The most obvious method is to increase the burning rate. The other alternative is to make the motor longer. A motor of high length-to-diameter (L/D) ratio will burn at a higher operating pressure and the net effect will be a higher specific impulse. Comparison of case 1 and case 3 demonstrates a 4.0% increase in specific impulse between the two, attributable to a 70% increase in length-to-diameter ratio.

At the same time, if case 5 and case 1 are compared, one sees that in spite of a lower L/D ratio and a slightly lower operating pressure, the 60.0-in.-long (case 1) unit outperformed case 5 and several of the other units in the group. This difference is assumed to be related to the length of the motor. The additional residence time of the metal particles in the longer motor allows more complete combustion of the aluminum ingredient.

Case 2 represents a straight cylinder without an IRR throat and shows a 6.0% lower performance than case 3 which is similar in size but does have an IRR throat.

Case 5 demonstrates that a higher L/D (7.6) will compensate for a lower web fraction (0.60) and still produce similar specific impulse at half the operating pressure.

Case 4 shows the effect of eliminating the exit cone. It was discovered in early firings that cutting a conical surface into the aft-face of a nozzleless grain not only prevented propellant break-off from the end of the bore, but also resulted in a 4-6% improvement in performance, despite the fact that propellant had to be removed to form an exit cone. This "exit" cone obviously provides an expansion surface and improves the recovery of kinetic energy during the early portion of the burn.

The motor in case 6 confirms that a lower L/D (6.1) reduces performance, although average pressure is the same and the web fraction is slightly higher than that of case 5.

Case 7 represents a 100-in.-long motor with a low web fraction of 0.40. This firing produced a more neutral pressure trace and maintained a higher average pressure. The result was performance only slightly lower than that of case 5, which had a similar L/D and a higher web fraction (0.60).

Case 8 verifies that although it exhibited a high average operating pressure, the low web fraction resulted in much lower performance than either case 2 or case 3 with similar L/D values. This motor is too short and pressure is too low to compensate for the low web fraction.

The plot of the specific impulse values on Fig. 3 shows cases 2, 3, and 8 falling in a straight line, indicating a linear relationship between average pressure and specific impulse at a fixed L/D ratio.

The second group of nine motors represent boosters loaded with reduced-smoke, nonmetallized/HTPB formulations, which yield theoretical specific impulse percentage values comparable to those produced by the first group. As expected, these motors without metal particles in the propellant display less sensitivity to motor size and L/D. It also appears that for these units, average operating pressure has more of an effect on operating efficiency than either residence time or motor length does for the first group.

Cases 13, 14, and 15 represent the same IRR configurations with three different propellant burn rates, and also exhibit a linear relationship between specific impulse and average pressure. Similarly, cases 9, 11, 12, and 16 show a parallel relationship but at a 3% lower impulse level. All four of these units exhibit lower impulse levels because they had relatively small (2-in.) exit diameters. The propellant exit cones of these motors did not allow them to take full advantage of higher initial expansion ratios, but in case 16 (S.C. even) this small cone yielded a 6.0% advantage over case 17, a similar unit without any exit cone.

§Percentage of specific impulse that a similar propellant would produce in a nozzled configuration.

Case 10 had a relatively low-burning-rate propellant and a lower web fraction, falling very low on the efficiency plot, and confirming a sharp drop in performance at lower pressures.

The last group of motors includes two zirconium propellant systems with a theoretical impulse that is much lower than that of the aluminum formulations. Comparison of cases 18 and 19 shows that a high L/D ratio barely compensates for a higher burning rate and operating pressure.

In summation, the evaluation of the data from this series of motors as well as over 200 others, leads to the following general conclusions:

1) For reduced-smoke propellant formulations, more efficient combustion and higher performance can be obtained with higher bruning rate and higher L/D ratio motors. However, optimum performance in comparison to a nozzled motor is most readily obtainable in a configuration that is short enough so that the nozzle section that has been replaced with propellant still represents a reasonable fraction of the total volume. Otherwise, the approximately 10% difference between the maximum specific impulse obtainable in a reduced-smoke nozzleless motor can not be compensated. This means that, unless the burning-rate pressure exponent of the propellant can be modified significantly, there is an increasing performance penalty inherent in either very short ($L/D < 3/1$) or very long ($L/D > 14/1$) nozzleless motors and performance ceases to be a significant advantage. Fortunately, such geometry extremes are usually eliminated for other reasons.

2) For metallized-propellant systems, there is evidently another important effect, namely particle combustion, which is related to residence time, chamber pressure, and motor size. All other things being equal, a full-scale motor loaded with metallized propellant will produce a higher specific impulse than a smaller motor, unless the metal particles are small enough to burn completely in a subscale motor.

Minor extrapolation of the specific impulse obtained with subscale aluminum-propellant motors indicates that specific impulse values in the range of 89% are obtainable with presently available propellants and that an additional 2-4% could be achieved by further tailoring the burning-rate exponent and the physical properties.

3) For zirconium-loaded systems, based on both nozzleless and nozzled motor data which exhibited a high dependence on motor size and average operating pressure,[5] it is expected that a full-size motor using existing propellant will produce 90% of the nozzled specific impulse and that the upper limit for an optimized system lies in the range of 91-92%.

4) As long as geometric extremes are avoided, all three of the major propellant systems allow a nozzleless design that will out-perform a nozzled version in a volume-limited system. The only probable penalty is that an optimum nozzleless motor may weigh up to 20% more than a comparable nozzled version for a high-density zirconium-loaded propellant system.

Additional Design Factors

The material presented in the previous section points out the basic relationship between motor performance, grain configuration, and propellant burning rate. However, besides the obvious constraints of combustor geometry and propellant burning rate, there are several additional factors that must be considered. Among them are the dependence of web fraction on propellant strain capacity, the propellant burning-rate pressure exponent, and the exact bore geometry.

As shown in the web fraction column, the motor gains listed in Table 2 cover a range of 0.40-0.70, which translates into a bore ratio (grain o.d./grain i.d.) of 1.67-3.3. As a general rule, a bore ratio of 3.0/1.0 will allow sufficient propellant loading to make a nozzleless motor comparable in performance. Higher bore ratio is desirable for improved performance but is limited by the structural capacity of the propellant. Again, in general terms, for a grain structure that has to operate at the typical $-65°$F low-temperature limit, the strain capacity must be 15% for a bore ratio of 3/1 and must increase proportionately to the ratio of the squares of the new value divided by the basic value of three:

$$\text{net strain} = 15\% \left(\frac{\text{bore ratio}}{3.0}\right)^2$$

Since strain capacities of 25% and more are readily achievable, it is possible to construct grains with ratios in excess of 3.50 but the calculation of bore ratio must include allowance for any elastic insulation layer. The layer must be included in the value of outside grain diameter to bore diameter multiple. Also, if peak operating pressure exceeds 1500 psi, the contribution of chamber pressure begins to have a significant effect on bore strain and must be included in the calculation.

Another major design variable is propellant burning-rate pressure exponent. As shown in Figs. 4 and 5, a reduction in the slope of the burning-rate curve has several positive effects. It decreases the ignition pressure value, thereby reducing structural loading and case maximum operating pressure (MEOP) limits, and increases the pressure and operating

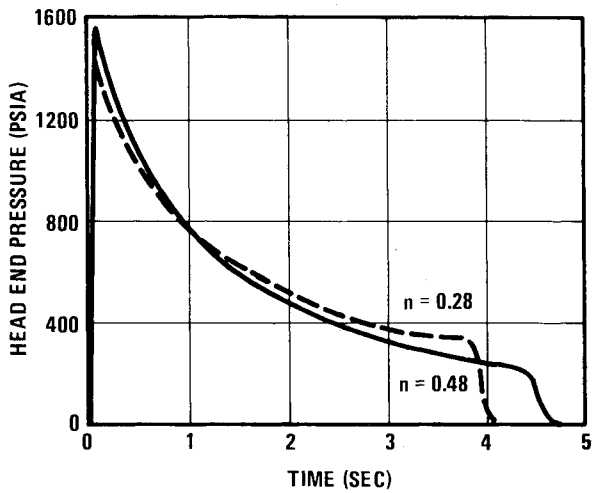

Fig. 4 Effect of propellant-pressure exponent on nozzleless IRR booster chamber pressure.

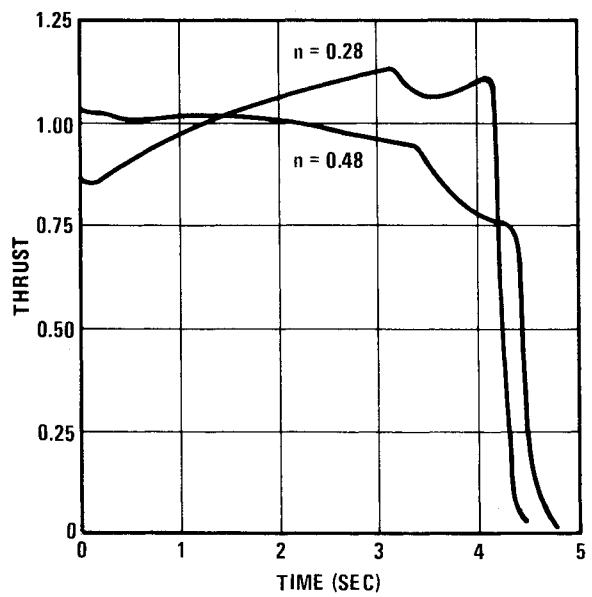

Fig. 5 Effect of propellant-pressure exponent on nozzleless IRR booster thrust.

Table 3 Model comparison of 7-in. booster performance

Parameter	Length, in.	Propellant weight, lbm	Burn rate at 1000 psia, in./s	Burn-rate exponent	I_{sp}[a], %	Bore ratio	Velocity change[a] %
Nozzled baseline	45.5	60	0.75	0.40	100	3.0	100
Baseline nozzleless	45.5	73	1.65	0.50	83	3.0	103
Higher burn rate	45.5	73	1.90	0.60	86	3.0	106
Higher web fraction	45.5	76	1.90	0.60	87	3.5	112
Lower-pressure exponent	45.5	76	1.90	0.40	88	3.5	113
Longer nozzled	55.5	72	0.65	0.40	100	3.0	100
Longer nozzleless	55.5	91	1.65	0.50	86	3.0	108
Shorter nozzled	35.5	48	0.90	0.45	100	3.0	100
Shorter nozzleless	35.5	55	1.65	0.50	78	3.0	92
	35.5	55	2.7	0.55	85	3.0	99

[a] Normalized specific impulse and velocity change.

Table 4 Model comparison of metallized propellant boosters

	Length, in.	Propellant weight, lbm	Bore ratio	I_{sp}, %	Velocity change, %
Baseline nozzled, aluminum	75.5	855	2.75	100.0	100.0
Baseline nozzleless, aluminum	77.0	1003	3.05	87.2	101.8
Baseline nozzleless, zirconium	69.5	1190	3.10	74.4	100.3
Longer Al nozzleless	87.5	1130	3.05	88.4	101.1
Longer Al nozzled	87.5	992	2.75	100.0	100.0
Longer Zr nozzleless	87.5	1476	3.10	76.8	108.4

efficiency during the last half of the firing. The result is a higher average operating pressure and more impulse. For a constant-diameter case design, the low slope will also make the thrust output more neutral.

In the case of a ramjet envelope, the ramjet nozzle will reduce the tailoff interval and can, in extreme cases, lead to a second unwanted peak pressure and thrust at the web burnout point.

The difference in pressure exponent over the operating pressure range of the two cases shown in the figures is 0.20. In this example, the net effect of the reduction in slope is a 3.0% gain in total impulse and a 7.0% reduction in the case maximum expected operating pressure (MEOP) of a 16-in. diameter, 85-in.-long IRR booster.

It is not always practical to railor a propellant to exhibit a significantly reduced exponent, but this variable should be put in the category of "desirable" nozzleless propellant characteristics, along with superior physical properties and a higher burning rate.

In addition to the previously listed primary variables, there are several secondary effects that are available for manipulation in order to make smaller adjustments in maximum pressure, burn time, and thrust neutrality. These are bore taper, propellant exit cone shape and length, and propellant elasticity. Because of the sensitivity of grain deformation to propellant properties, it may be feasible under some circumstances to modify the propellant physical properties in order to produce minor changes in ballistics. This grain-elasticity dependence also manifests itself as a lower temperature sensitivity in nozzleless designs. Because the bore forms the nozzle, at the high temperature, the propellant deforms more and opens the bore to partially compensate for the higher propellant burn rate. At the lower temperatures, the increased stiffness of the propellant keeps the bore smaller and partially compensates for the lower propellant burning rate.

The result is that nozzleless motors typically exhibit only 50-65% of the operating temperature sensitivity of nozzled motors.

Performance Optimization

Although the empirical nozzleless booster data available do not cover all of the extremes in configuration and propellant ballistics that are of interest, there are sufficient motor data to allow reasonable extrapolation from the norms represented by the motor data.

The following section discusses the predicted behavior of three different IRR booster systems with the objective of comparising the performance of baseline nozzled boosters against state-of-the-art and "optimized" nozzleless configurations fitting within the same combustor envelopes.

Reduced Smoke System

The first configuration, the behavior of which is summarized in Table 3, represents a reduced-smoke propellant, 7.0-in. diameter, integral-ramjet booster with a nominal length of 45 in. A nozzleless state-of-the-art version of this booster will weigh about 4 lb less, will utilize a propellant with twice the burn rate, and will produce a 3% higher velocity increment with an average specific impulse which is 83% of that produced by the nozzled version.

The increase in performance of this nozzleless design over the comparable nozzled design depends on how much the propellant can be modified. An existing version of this propellant with a burning rate 2.5 times as high can be used to increase the performance advantage to 5.5%. At the same time, taking full advantage of the 25% strain capacity demonstrated by this propellant, the bore could be closed down to a ratio of 3.5/1.0. This would allow loading of 3 lb more of propellant and would produce a net performance increase of 12.4%. Making both changes simultaneously would drive the MEOP required back up to match that of the nozzled design, and the only penalty would be a net weight increase of about 2% in the missile weight. Table 3 summarizes the results of these iterations as well as the effect of length changes on the specific impulse developed.

A motor with a pressure exponent reduced from 0.50 to 0.40 would produce a net advantage of 13% for a nozzleless design over a comparable nozzled design.

As discussed in the previously presented material, changes in motor length and exact grain bore shape can also be manipulated. If the design is not limited to a specific combustor geometry, then one can substitute grain diameter and length changes for burn-rate and web fraction variation, with the understanding that higher L/D motors require a lower burning rate, that specific impulse will be almost linear with average pressure, and that a change to any of the design variables will inevitably require that others be modified in order to maintain optimum conditions.

As Table 3 shows, longer motors with higher L/D ratios would allow higher operating pressures and higher specific impulse. A 10-in. length increase in the baseline combustor geometry yields an 8% advantage in velocity over the larger nozzled unit, indicating that the initial 6.5/1.0 length-to-diameter ratio is far short of optimum nozzleless motor length. Subsequent burn-rate and bore changes could increase the difference to at least the same 14% as shown for the baseline length but factors such as maximum operating pressure, minimum burn time, and other operational constraints would realistically limit the net increases to the range of 10-14%. By extrapolating the data presented in Fig. 3, it can be shown that a relative specific impulse in excess of 89.5% can be obtained only by allowing average operating pressures in the range of 1200 psia. Since such a value represents the practical booster structure limit, any further increases would require significant improvement in burning-rate pressure exponents.

The last set of entries in Table 3 show the disadvantages of lower L/D ratio combustor geometry. A 10-in.-shorter nozzleless unit does not come close to matching the nozzled design unless the burning rate is increased significantly.

Metallized Propellant Systems

Referring to Fig. 3, it is apparent that for metallized-propellant systems, a variable other than average operating pressure determines the net performance of a nozzleless booster. The motors exhibiting high performance at lower operating pressures are typically longer.

Absolute size must therefore be taken into account and where full scale motor data are lacking the available data must be extrapolated. Although the data for cases 2, 3, and 8 show a much higher response to increases in operating pressure than that exhibited by the smaller reduced-smoke motors, it is not probable that the specific impulse delivered by the larger (over 12-in. diameter, $L/D > 4.0$) motors will fall on a parallel line drawn through case 5. Initial particle size, residence time, and theoretical thermochemistry calculations indicate that for the current aluminized-propellant systems, 90% of the normalized specific impulse at an average operating pressure of 1000 psia, probably represents the upper limit.

Table 4 lists a number of major size iterations for a nominal 19-in. diameter, 80-in.-long booster loaded with either Al/HTPB or Zr/HTPB propellant. The first three cases compare an aluminum- and a zirconium-loaded nozzleless design with the control variable being a specified velocity increment. The data indicate that comparable performance is achievable, but at the expense of total launch weight. A shorter, heavier zirconium-propellant nozzleless motor demonstrates the concept that high-density propellant provides volumetric efficiency.

The last three entries compare three similar but longer motors and show that the zirconium-loaded nozzleless motor outperforms the nozzled motor by 8.4%, with a net weight penalty, including the inert-weight difference, of about 19.0%. This indicates that a shorter zirconium motor would produce comparable performance with a weight penalty of about 10%.

Again, it can be seen that at the higher L/D ratio the nozzleless design does become more efficient and that if one took a large motor with a L/D ratio of more than 6/1, the nozzleless design would show increases in specific impulse to a value above 90% of the reference specific impulse in each case.

The configurations considered in this paper consist of IRR boosters with ramjet nozzle exit cones limited to the diameter of the motor case. Configurations that allow expansion cones extending outside the case diameter will allow additional propellant loading and kinetic-energy recovery, and can be expected to show a 10-15% advantage in performance over nozzled motors which can not take full advantage of the available volume.

Summary and Conclusions

The concept of a nozzleless solid-propellant rocket motor offers a number of advantages over conventional nozzled designs, but nowhere does the application of a nozzleless motor fit more logically than in the case of an integral ramjet system. Here the relative simplicity, volumetric efficiency, and mass fraction advantage of a nozzleless booster offer distinct advantage over the ejectable nozzle design.

The one factor that could limit the usefulness of the nozzleless booster design is the question of performance comparability. The data presented in this paper confirm within a reasonable range of length-to-diameter ratios, a nozzleless IRR booster will readily match or outperform a nozzled design with comparable external geometry. When one considers the benefits of eliminating the ejectable nozzle with its attendant weight, reliability, and debris hazard penalties, the relatively simple nozzleless design appears to be the logical choice for most IRR booster applications.

References

[1] Small, K.R. and Taylor, D.E., "Nozzleless Rocket Motor Demonstration Program," AFRPL-TR-74-17, Contract F04611-73-C-0052, April 1979.

[2] Platzek, H.M. and Feist, R.W., "Air Launch-Low Volume Ramjet (ALVRJ) Booster Motor Development and Flight Testing" (U), 1976 JANNAF Propulsion Meeting. Confidential.

[3] Harry, D.P., Price, C.F., Small, K.R., and Taylor, D.E., "Nozzleless Rocket Motor Internal Ballistics Computer Program," AFRPL-TR-73-20, Mar. 1973.

[4] Procinsky, I.M., Harry, D.P., Clement, J.A., Markle, R.J., and Smith, W.R., "Revised Users Manual for the Nozzleless Rocket Motor Internal Ballistics Computer Program," AFRPL-TR-78-82, Jan. 1979.

[5] Fields, J.L., Martin, J.D., and Larimer, M., "Development of High Density-Impulse Solid Propellants for Air Launch Motor Application" (U), AFRPL-TR-77-3, Contract F04611-74-C-0044, Nov. 1976.